



Argonne National Laboratory, a U.S. Department of Energy Office of Science laboratory, is operated by The University of Chicago under contract W-31-109-Eng-38.

**DISCLAIMER**

This report was prepared as an account of work sponsored by an agency of the United States Government. Neither the United States Government nor any agency thereof, nor The University of Chicago, nor any of their employees or officers, makes any warranty, express or implied, or assumes any legal liability or responsibility for the accuracy, completeness, or usefulness of any information, apparatus, product, or process disclosed, or represents that its use would not infringe privately owned rights. Reference herein to any specific commercial product, process, or service by trade name, trademark, manufacturer, or otherwise, does not necessarily constitute or imply its endorsement, recommendation, or favoring by the United States Government or any agency thereof. The views and opinions of document authors expressed herein do not necessarily state or reflect those of the United States Government or any agency thereof.

Available electronically at <http://www.osti.gov/bridge/>

Available for a processing fee to U.S. Department of Energy and its contractors, in paper, from:

U.S. Department of Energy  
Office of Scientific and Technical Information  
P.O. Box 62  
Oak Ridge, TN 37831-0062  
phone: (865) 576-8401  
fax: (865) 576-5728  
email: [reports@adonis.osti.gov](mailto:reports@adonis.osti.gov)

A FINITE DIFFERENCE MODEL USED TO PREDICT THE CONSOLIDATION OF A  
CERAMIC WASTE FORM PRODUCED FROM THE ELECTROMETALLURGICAL  
TREATMENT OF SPENT NUCLEAR FUEL

by

K. J. Bateman and D. D. Capson

Engineering Technology Division  
Argonne National Laboratory-West  
P. O. Box 2528  
Idaho Falls, ID 83403-2528

NT TECHNICAL MEMORANDUM NO. 209

Results reported in the NT-TM series of memoranda frequently are preliminary and subject to revisions. Consequently they should not be quoted or referenced.



## TABLE OF CONTENTS

	<u>Page</u>
ACRONYMS.....	v
ABSTRACT.....	vii
1. Introduction.....	1
2. Experimental Description .....	1
3. Computer Model Description .....	3
4. Model 1 Results .....	11
5. Model 2 Results .....	13
6. Conclusions.....	18
ACKNOWLEDGMENT .....	18
REFERENCES .....	19
APPENDIX .....	20

## LIST OF FIGURES

	<u>Page</u>
1. Geometry of 25 kg Experimental Canister and Top Plate .....	2
2. Geometry of CWF and Mesh of Plane A.....	7
3. Bulk Density Versus Soak Time for Ceramic Waste Form.....	8
4. Experiment Setup of Linear Potentiometer .....	9
5. Height of Production Canister Versus Ceramic Waste Form Mass .....	11
6. Ceramic Waste Form Temperature Versus Mass .....	12
7. Production Size Ceramic Waste Form Core Temperature Versus Time .....	12
8. Temperature Versus Time for 25 kg Ceramic Waste Form Model .....	13
9. Bulk Density Versus Time for the 25 kg Ceramic Waste Form Model .....	14
10. Experimental Data from 25 kg Ceramic Waste Form Experiment.....	14
11. Comparison of Model 2 Versus 25 kg Experimental Temperature Data .....	15
12. Comparison Model 2 Versus 25 kg Experimental Bulk Density Data .....	16
13. Comparison of Model 2 Versus 140 kg Experimental Temperature Data .....	17
14. Comparison of Model 2 Versus 140 kg Experimental Bulk Density Data .....	18

## ACRONYMS

ANL	Argonne National Laboratory
ANL-East	Argonne National Laboratory-East
ANL-West	Argonne National Laboratory-West
EBR-II	Experimental Breeder Reactor-II
CMT	Chemical Technology Division
CWF	Ceramic Waste Form
EDL	Engineering Development Laboratory
HFEF	Hot Fuel Examination Facility
PC	Pressureless Consolidation

## LIST OF SYMBOLS

Bi	Biot Number
C	Concentration
$C_0$	Initial Concentration
$C_p$	Heat Capacity
$C_r$	Constant for Infinite Cylinder Exact Solution Equation
E	Activation Energy/Universal Gas Constant
$F_0$	Fourier Number
i	Nodal Coordinate in Axial Direction
j	Nodal Coordinate in Radial Direction
$J_0$	Bessel Function of Order 0
$J_1$	Bessel Function of Order 1
k	Thermal Conductivity
L	Length
p	Time Step Number
R	Radius
r	Dimensionless Radius
T	Temperature
t	Time
x	Dimensionless Height
<b>Greek</b>	
$\alpha$	Thermal Diffusivity
$\beta$	Order of Temperature
$\Delta r$	Distance Between Radial Nodes
$\Delta z$	Thermal Diffusivity
$\theta$	Dimensionless Temperature
$\rho$	Density
$\zeta_r$	Positive Roots of a Transcendental Equation for an Infinite Cylinder
$\zeta_x$	Positive Roots of a Transcendental Equation for a Plane Wall

A FINITE DIFFERENCE MODEL USED TO PREDICT THE CONSOLIDATION OF A  
CERAMIC WASTE FORM PRODUCED FROM THE ELECTROMETALLURGICAL  
TREATMENT OF SPENT NUCLEAR FUEL

by

K. J. Bateman and D. D. Capson

ABSTRACT

Argonne National Laboratory (ANL) has developed a process to immobilize waste salt containing fission products, uranium, and transuranic elements as chlorides in a glass-bonded ceramic waste form. This salt was generated in the electrorefining operation used in the electrometallurgical treatment of spent Experimental Breeder Reactor-II (EBR-II) fuel. The ceramic waste process culminates with an elevated temperature operation. The processing conditions used by the furnace, for demonstration scale and production scale operations, are to be developed at Argonne National Laboratory-West (ANL-West). To assist in selecting the processing conditions of the furnace and to reduce the number of costly experiments, a finite difference model was developed to predict the consolidation of the ceramic waste. The model accurately predicted the heating as well as the bulk density of the ceramic waste form. The methodology used to develop the computer model and a comparison of the analysis to experimental data is presented.



## 1. Introduction

Argonne National Laboratory (ANL) developed a process to immobilize the waste salt stream from the electrometallurgical treatment of spent Experimental Breeder Reactor-II (EBR-II) fuel in a glass-bonded ceramic waste form [1]. The waste salt stream consisted of spent electrolyte (LiCl-KCl eutectic) containing alkali, alkali earth, lanthanide, and actinide fission products present as chloride salts. In making the ceramic waste form, these halides were first occluded into the pores of zeolite-4A using an elevated temperature blending process. Salt loaded zeolite was then mixed with glass frit and loaded into cylindrical stainless steel canisters. Finally, they were subjected to elevated temperature in a furnace. The resulting ceramic waste form (CWF) was a glass-bonded sodalite suitable for long-term storage in a repository.

The Chemical Technology Division (CMT) at Argonne National Laboratory-East (ANL-East) performed initial development tests for this process. Lab-scale experiments were performed using relatively small sample sizes of 20 g. These experiments have shown that a process time of 8 to 24 hours at greater than 900°C results in a densification of 2:1. It has been recommended that a temperature of 915°C be used to optimize the procedure [2]. At Argonne National Laboratory-West (ANL-West), the process was scaled-up to produce demonstration-scale CWF (up to 150 kg), and will eventually be used for CWF production-scale (greater than 150 kg). The demonstration-scale effort included processing of nonirradiated material in the Engineering Development Laboratory (EDL) and continued with processing of irradiated material in the Hot Fuel Examination Facility (HFEF). Eventually, the production-scale effort will follow a similar path. To assist in selecting the operating conditions of the furnace and to reduce the number of costly experiments, a finite difference model was developed to predict the consolidation of the ceramic waste. The details of this model and a comparison with experimental data will be the primary focus of this report.

## 2. Experimental Description

Each experiment consisted primarily of CWF material contained in a stainless steel can, that was processed (soaked) in a furnace at 915°C. A stainless steel plug rested on top of the waste material to level the surface of the material. The plug applied a load of approximately 1-psi. Thermocouples were placed in strategic locations within the waste material in order to measure temperature. To measure the vertical displacement, a linear potentiometer was placed on top of the plug. Since the geometry of each experiment was cylindrical, and radius remains constant, vertical displacement measured by the potentiometer was directly related to the material's volume and density.

$$V = H \cdot \pi \cdot R^2 \quad (1)$$

where:

$V$  = volume (m<sup>3</sup>)

$H$  = height (m)

$R$  = radius (m)

and

$$\rho = M/V \quad (2)$$

where:

$\rho$  = density of material (kg/m<sup>3</sup>)

$M$  = mass of material (kg)

After various small-scale experiments were conducted to obtain initial thermophysical data, a 25 kg experiment was conducted to test the computer model, specifically thermal conductivity ( $k$ ), density ( $\rho$ ), and heat capacity ( $C_p$ ). A stainless steel can with an inner radius of 12.4 cm and a height of 61 cm was filled with 25 kg of salt-loaded zeolite/glass mixture. The can was tapped for 5 min resulting in a green geometric density of 0.91 g/cm<sup>3</sup>. Three 1.6 mm thermocouples were inserted through thermal wells located in the bottom of the can to heights of 15.25 cm, 22.8 cm, and 15.25 cm, respectively. The first two were located in the center of the can radially, whereas the third was located 8.9 cm from the radial center (Fig. 1a). A fourth thermocouple was spot welded onto the outside surface of the can and was used as the furnace control thermocouple. A 3.175 mm thick stainless steel plate was placed on top of the material. To keep the top surface level, four additional weights, totaling 24.75 kg, were placed on top of the top plate (Fig. 1b). The can and material were placed in a furnace with internal working dimensions of 61 cm x 61 cm x 76 cm. A linear potentiometer with a measuring range of 60 cm was mounted above the furnace with an attached 6.35 mm stainless steel rod protruding through a hole centered in the ceiling of the furnace and resting on the top plate of the can (Fig. 1b). The furnace was ramped from room temperature to 500°C at 5°C/min. The furnace was held at 500°C for 30 hours and then ramped to 915°C at 1°C/min. The furnace held at 915°C for 48 h and then was shut off.

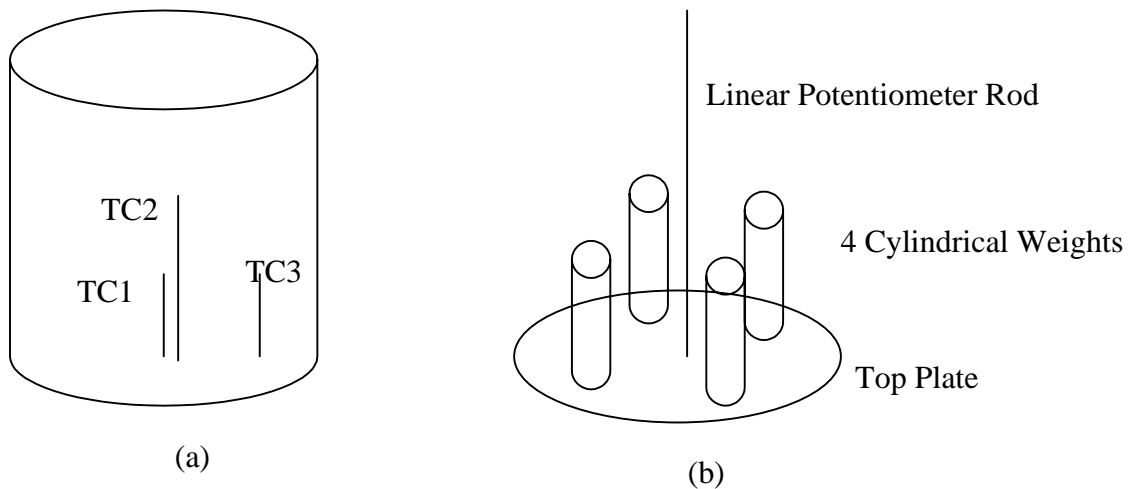


Fig. 1. (a) Geometry of 25 kg Experimental Canister and (b) Top Plate

### 3. Computer Model Description

Two separate computer models were developed to predict densification rates for given CWF mass and soak times. The first model used exact solution equations and constant properties in order to bound soak times between best and worst case scenarios. The second model used transient, finite difference equations to incorporate changing thermophysical properties during processing. Both models were created using the software package MathCad 2001 [3].

The first model was based on the following equations. First, assuming a planar wall is [4]:

$$\theta_x = \sum_{n=1}^{\infty} C_{x_n} \cdot \exp[-(\zeta_{x_n})^2 \cdot Fo] \cdot \cos(\zeta_{x_n} \cdot x) \quad (3)$$

where:

$\theta$  = dimensionless temperature

$x$  = dimensionless height

$\zeta$  = positive root

$Fo$  = Fourier Number =  $\alpha t/L^2$

$t$  = time (s)

$L$  = length (m)

$\alpha$  = thermal diffusivity, defined as  $k/\rho \cdot C_p$  ( $m^2/s$ )

$k$  = thermal conductivity ( $W/m \cdot K$ )

$C_p$  = heat capacity ( $J/kg \cdot K$ )

$C_{x_n}$ , a constant for the plane wall exact solution, is:

$$C_{x_n} = \frac{4 \sin(\zeta_{x_n})}{2\zeta_{x_n} + \sin(2 \cdot \zeta_{x_n})} \quad (4)$$

And the discrete values (eigenvalues) of  $\zeta_{x_n}$  are positive roots of the transcendental equation:

$$\zeta_{x_n} \cdot \tan(\zeta_{x_n}) = Bi \quad (5)$$

Secondly, assuming an infinite cylinder, [4]

$$\theta_r = \sum_{n=1}^{\infty} C_{r_n} \cdot \exp[-(\zeta_{r_n})^2 \cdot Fo] \cdot J0(\zeta_{r_n} \cdot r) \quad (6)$$

where  $Fo = \alpha \cdot t/R^2$  and  $C_{r_n}$  is:

$$C_{r_n} = \frac{2}{\zeta_{r_n}} \cdot \frac{J1(\zeta_{r_n})}{J0(\zeta_{r_n})^2 + J1(\zeta_{r_n})^2} \quad (7)$$

and the discrete values of  $\zeta_{r_n}$  are positive roots of the transcendental equation:

$$\zeta_{r_n} \cdot \frac{J1(\zeta_{r_n})}{J0(\zeta_{r_n})} = Bi \quad (8)$$

where the quantities  $J1$  and  $J0$  are Bessel functions of the first kind and  $\theta$  is a dimensionless temperature parameter which is equal to the product of  $\theta_x$  and  $\theta_r$  [4].

$$\theta = \theta_x \times \theta_r = (T - T_{\infty}) / (T_i - T_{\infty}) \quad (9)$$

where:

$T$  = temperature (K)

The  $x$  and  $r$  represent dimensionless positions as  $x$  = height/total height and  $r$  = radius/total radius. The model was based on the assumption that the Biot number ( $Bi$ ) was infinite or, in other words, the surface temperature was equal to the furnace temperature.

The equations used in model 1 represent exact solutions for constant property analysis [4]. However, to successfully model a transient process with varying properties, a different approach was needed. Model 2 (Appendix A) utilized a finite difference approximation in order to incorporate varying properties, i.e., thermal conductivity, density, and heat capacity, into the model. This model was created to predict processing conditions necessary to achieve the desired consolidation of the CWF and utilized fundamental heat transfer equations [5]. The first equation (10), Fourier's law states that:

$$q/A = -k \cdot \nabla T \quad (10)$$

where:

$q$  = heat flux (W)

$A$  = area (m<sup>2</sup>)

$T$  = temperature (K)

$\nabla$  = Del operator (for cylindrical coordinates  $\nabla = i \, d/dr + j \, 1/r \, d/d\theta + k \, d/dz$ )

The second equation utilized is the conservation of energy (Eq. 11) shown below.

$$E_{in} + E_g - E_{out} = E_{st} \quad (11)$$

where:

$E_{in}$  = entering energy (W)

$E_g$  = generated energy (W)

$E_{out}$  = exiting energy (W)

$E_{st}$  = stored energy (W)

The entering and exiting energy terms are represented by Fourier's law Eq. (10). The generation and storage terms are represented by Eqs. (12) and (13), respectively.

$$E_g = q_g dV \quad (12)$$

$$E_{st} = \rho \cdot C_p dT/dt \, dV \quad (13)$$

where:

$q_g$  = generated heat (W/m<sup>3</sup>)

The generation heat term ( $q_g$ ) can be further reduced into separate heat generating terms as shown by Eq. (14).

$$q_g = q_{rad} + q_{Hr} + q_{PV} \quad (14)$$

where:

$q_{rad}$  = generation due to radioactivity (W/m<sup>3</sup>)

$q_{Hr}$  = generation due to heat of reaction (W/m<sup>3</sup>)

$q_{PV}$  = generation due to pressure-volume work (W/m<sup>3</sup>)

Combining Eqs. (10) through (14), the general form of the heat equation in cylindrical coordinates is

$$\frac{1}{r} \cdot \frac{\partial}{\partial r} \left( k \cdot r \cdot \frac{\partial T}{\partial r} \right) + \frac{1}{r^2} \cdot \frac{\partial}{\partial \theta} \left( k \cdot \frac{\partial T}{\partial \theta} \right) + \frac{\partial}{\partial z} \left( k \cdot \frac{\partial T}{\partial z} \right) + q_{rad} + q_{Hr} + q_{PV} = \rho \cdot C_p \cdot \frac{\partial T}{\partial t} \quad (15)$$

Making the assumptions that thermal conductivity (k) varies with time and not with position, and that there are no gradients in the  $\theta$  direction, Eq. (15) can be simplified to Eq. (16).

$$\frac{1}{\alpha} \cdot \frac{\partial T}{\partial t} = \frac{1}{r} \frac{\partial}{\partial r} \left( r \cdot \frac{\partial T}{\partial r} \right) + \frac{\partial^2 T}{\partial z^2} + \frac{q_{rad}}{k} + \frac{q_{Hr}}{k} + \frac{q_{PV}}{k} \quad (16)$$

Defining the parameter  $p$  as the time step number

$$p = t / \Delta t \quad (17)$$

then utilizing the definition of  $p$ ,  $dT/dt$  becomes

$$\frac{dT}{dt} = \frac{T(p+1)_{i,j} - T(p)_{i,j}}{\Delta t} \quad (18)$$

then Eq. (16) becomes Eq. (19).

$$(T_{p+1})_{i,j} = \alpha \cdot \Delta t \cdot \left[ \begin{aligned} & \frac{(T_p)_{i+1,j} + (T_p)_{(i-1),j} - 2 \cdot (T_p)_{i,j}}{\Delta z^2} \dots \\ & + \frac{(T_p)_{i,j+1} + (T_p)_{i,j-1} - 2 \cdot (T_p)_{i,j}}{\Delta r^2} \dots \\ & + \frac{1}{r} \cdot \frac{(T_p)_{i,j-1} - (T_p)_{i,j+1}}{2 \cdot \Delta r} + \frac{q_g}{k} \end{aligned} \right] + (T_p)_{i,j} \quad (19)$$

where:

- $p$  = time step number ranging from 0 to the defined number of time steps
- $i$  = node number in the z direction
- $j$  = node number in the r direction
- $\Delta t$  = length of time step p (s)

$\Delta z$  = distance between nodes in z direction (m)  
 $\Delta r$  = distance between nodes in the r direction (m)

The parameters  $\Delta z$  and  $\Delta r$  are the distances between axial and radial nodes, respectively, as shown in Fig. 2. They are calculated by the user-input number of nodes in each direction. The greater the number of nodes, the smaller  $\Delta z$  and  $\Delta r$  become. Larger values of nodes served to increase accuracy, but also greatly increased computation time.

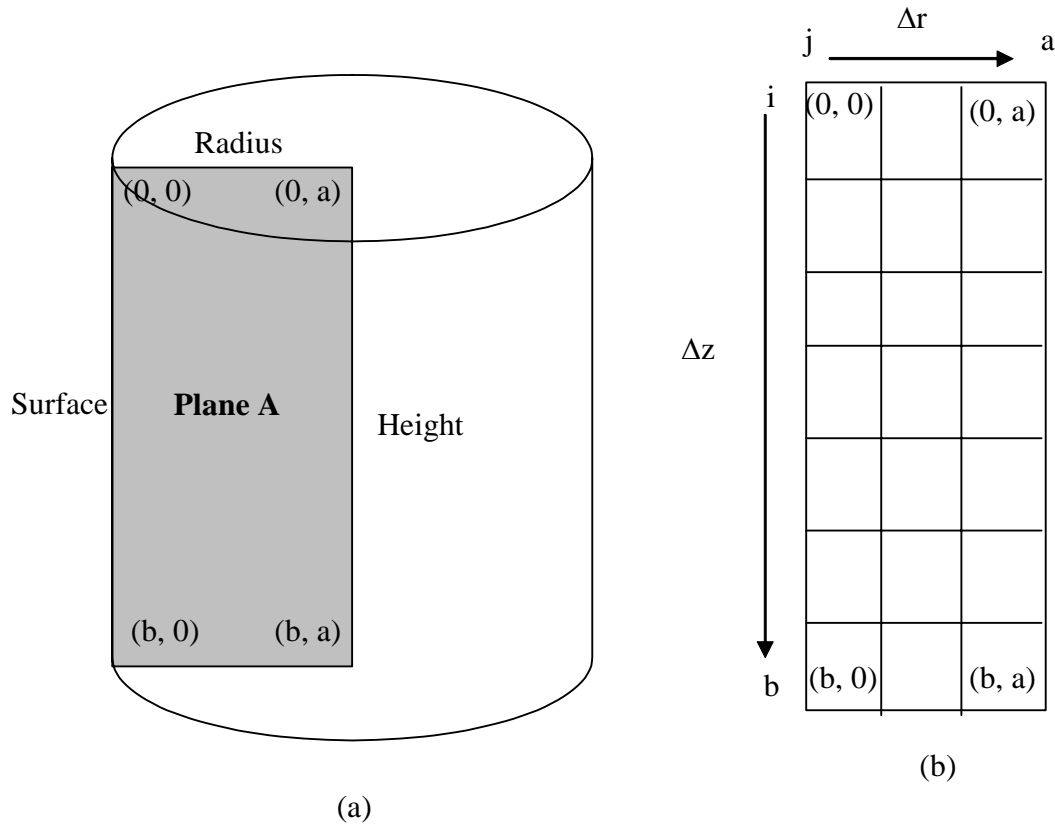


Fig. 2. (a) Geometry of CWF and (b) Mesh of Plane A

Equation (19) defines the temperature at an interior node of coordinates  $i$  and  $j$ . Each intersection, as shown in Fig. 2, represents a node of coordinates  $i, j$ ;  $i$  represents the number of nodes from the top and  $j$  represents the number nodes from the cylinder surface. As shown in Eq. (19), the temperature at time step  $p+1$  is determined primarily by the temperatures of the previous time step ( $p$ ). Once initial conditions and boundary conditions are applied, Eq. (19) can be used to calculate the temperature at each node. The initial conditions that need to be specified are: (a) the dimensions of the processing can, (b) the mass of ceramic waste to be processed, (c) the number of nodes the model should use to accurately represent the process, and (d) the initial temperature. The boundary conditions, that need to be specified, are: (a) ramp up rates, (b) hold temperatures, (c) soak times, and (d) run time of model.

During the sintering process of the CWF all of the thermophysical properties ( $k$ ,  $C_p$ , and  $\rho$ ), which define thermal diffusivity ( $\alpha$ ), vary with temperature and with time at temperature. To obtain relationships to approximate waste form density, experimental data was analyzed. The primary source of this density data was experiments conducted at ANL-East by Mark Hash [2]. The symbols in Fig. 3 show the densification data for different temperatures versus soak time.

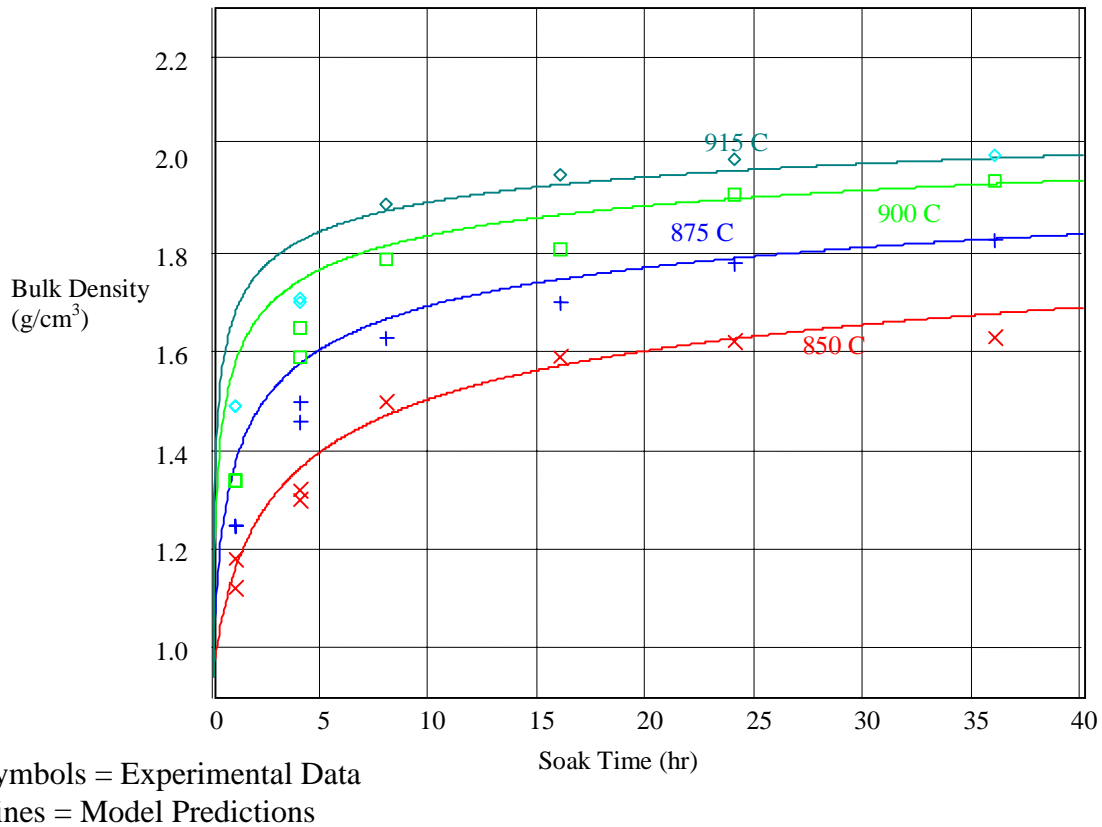


Fig. 3. Bulk Density Versus Soak Time for Ceramic Waste Form

Unfortunately, the thermal conductivity ( $k$ ) and the heat capacity ( $C_p$ ) could not be measured during processing. However, the density ( $\rho$ ) could be continuously measured using an experimental apparatus utilizing a linear potentiometer, see Fig. 4. By observing how density changed during the sintering process, the behavior of  $k$  and  $C_p$  could be estimated. To match this data, a chemical reaction equation was used. A single species, sixth order reaction converting “species 1” (salt loaded zeolite/glass powder) to “species 2” (consolidated sodalite/glass solid) was fit to the experimental 20 g sample densities, as is shown by the symbols in Fig. 3. The equations used to generate the model data, shown as solid lines in Fig. 3, are based on a temperature dependent Arrhenius equation as given by Eq. (20) [6].



Fig. 4. Experiment Setup of Linear Potentiometer

$$\rho = \rho_i \cdot \left[ 1 + \left( \frac{\rho_{th}}{\rho_i} - 1 \right) \cdot \left[ X_0 - \left[ X_0^{1-n} + A_0 \cdot \left( \frac{T}{K} \right)^\beta \cdot \exp\left( \frac{-E_a}{T} \right) \cdot t \cdot (n-1) \right]^{\frac{1}{1-n}} \right] \right] \quad (20)$$

where

$\rho_i$  = initial density (kg/m<sup>3</sup>)

$\rho_{th}$  = theoretical density (kg/m<sup>3</sup>)

$X_0$  = initial weight percent of unconsolidated material

$A_0$  = rate constant (1/s)

$T$  = temperature (K)

$\beta$  = order of temperature

$E_a$  = activation energy (K)

$t$  = time (s)

$n$  = reaction order

Using the data that best fit the experimental data, the value of rate constant ( $A_0$ ) was  $1 \times 10^{-5}$  Hz, order of temperature ( $\beta$ ) was 5.159, and activation energy ( $E$ ) was  $3.9 \times 10^4$  K.

Using Eq. (20), the density ( $\rho$ ) can be calculated for each temperature given by Eq. (19). The bulk density can then be calculated by weighting the density at each node by its radial position in the cylinder. The height of the cylinder is then calculated using the average density. Since the height changes, the parameter  $\Delta z$  must also be recalculated at each time step.

Heat capacity of solids generally follows the convention of varying only with temperature. The sample densities data, the symbols in Fig. 3, suggests that the heat capacity for the CWF is consistent with this general rule [7]. The temperature dependence was found to fit the form shown by Eq. (21).

$$C_p = \frac{a}{T^2} + b \cdot T + c \quad (21)$$

Where a, b, and c are constants found by fitting experimental data. The values of a, b, and c were found to be: 772.318, 0.535, and  $-9.494 \times 10^6$ , respectively.

The thermal conductivity (k) was assumed to vary with temperature and density. The temperature and density dependence are shown by Eq. (22).

$$k = \frac{\rho_i \cdot (k_{ref} - k_i)}{\rho_{ref} - \rho_i} \cdot \frac{\rho - \rho_i}{\rho_i} + T \cdot \frac{k_{int} - k_i}{T_{ref} - T_i} + k_i - T_i \cdot \frac{k_{int} - k_i}{T_{ref} - T_i} \quad (22)$$

where:

$k_{ref}$  = post processing measured thermal conductivity value (W/m·K)

$k_i$  = initial thermal conductivity value (W/m·K)

$\rho_{ref}$  = post processing density, corresponding to  $k_{ref}$  ( $\text{kg/m}^3$ )

$K_{int}$  = estimated thermal conductivity value at  $T_{ref}$  (W/m·K)

$T_{ref}$  = softening point of the glass in ceramic (K)

$T_i$  = initial temperature (K)

The initial value of thermal conductivity of 0.135 W/m/K was obtained from experiments performed by Purdue University[7]. The softening point, or transition point, of the glass is the temperature where the glass begins to soften. For the glass used in these experiments, this value was 567°C. Up to the transition point, the value for thermal conductivity was set in the model to increase linearly to 1.5 times the initial value. After the transition point was reached, the value was set to increase proportionally with the calculated density. The value continued to increase until the thermal conductivity reached a maximum of 1.4 W/m/K, corresponding with a calculated density of  $2 \text{ g/cm}^3$ . Setting the boundary temperature and then solving for time at temperature related properties, the model solved Eq. (19) to predict material temperature as a function of location, and Eq. (20) was used to predict densification.

#### 4. Model 1 Results

The results of Model 1 may primarily be used to address criteria with the overall design. The criteria addressed include optimal production-scale processing size, the affect processing size has on heat up and soak times, and optimal can dimensions for production-scale processing. The optimal radius of the CWF storage can is approximately 10.2 in. (25.9 cm). Using the fixed radius and setting the bulk density equal to the initial and the final bulk densities, the model can solve for the bounding heights of a CWF canister (Fig. 5). The graph depicts the fact that the when the final density value was used, a shorter cylinder height will be needed to contain the CWF. The graph also illustrates the range of possible can heights needed for production-scale processing.

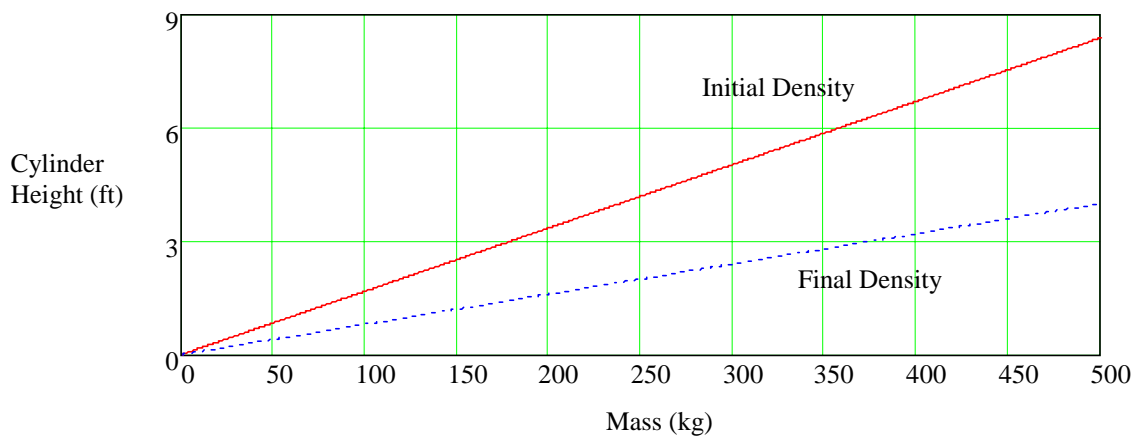


Fig. 5. Height of Production Canister Versus Ceramic Waste Form Mass

Fig. 6 shows the core temperature (using all initial thermophysical properties) versus mass of the CWF for different soak times at 915°C. The graph represented in Fig. 6 indicates that for masses greater than 200 kg, the core temperature is independent of mass. Since radius is held constant, once a certain mass/height is attained, the core is heated almost entirely from the sides; i.e., radially. For masses greater than 200 kg, the temperature cycle required is independent of mass.

Fig. 7 shows the difference in core heating profiles using final values of  $k$ ,  $\rho$ , and  $C_p$ . Similar data is presented using initial values of  $k$ ,  $\rho$ , and  $C_p$ . As illustrated in Fig. 7, the temperature cycle required to allow the core to reach 800°C ranges from 12 h to 70 h. The actual core heat up time will be between these two extremes, depending on how and when the thermophysical properties change.

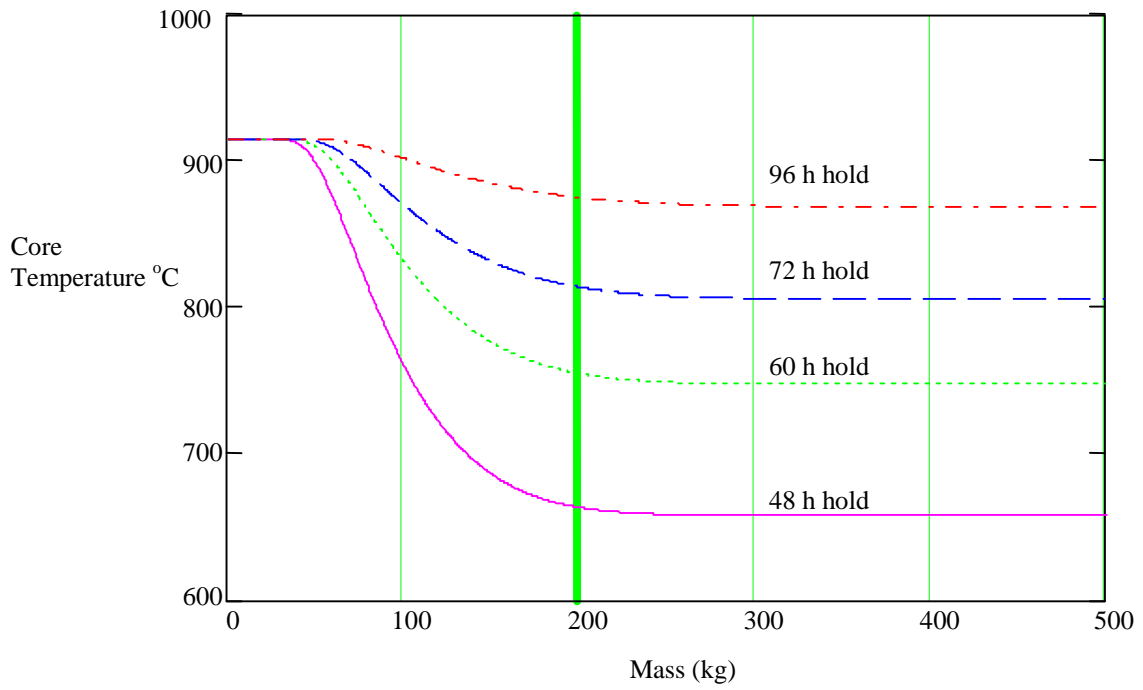


Fig. 6. Ceramic Waste Form Temperature Versus Mass

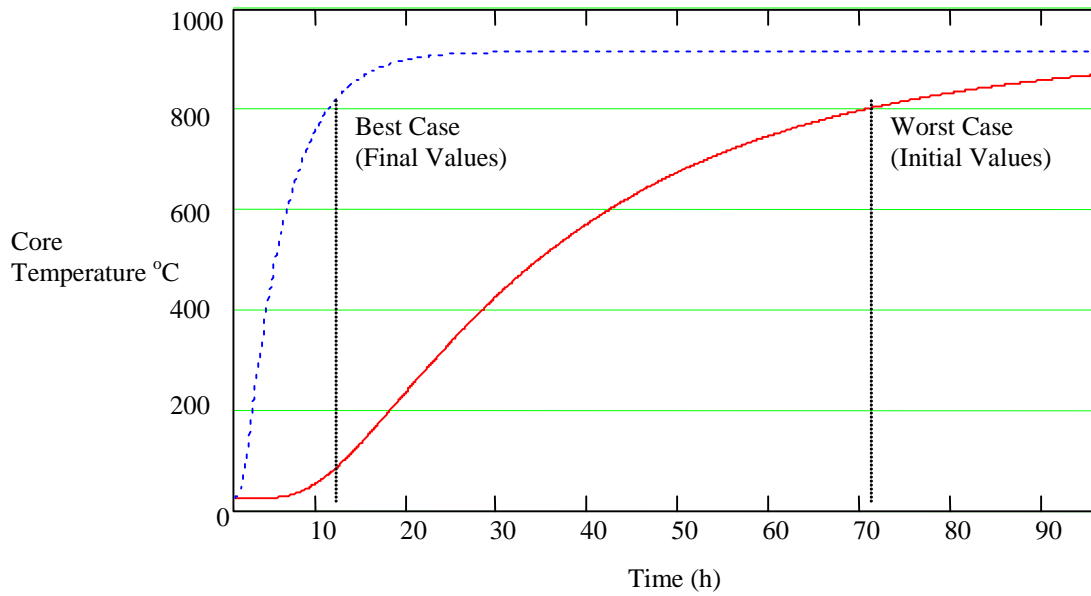


Fig. 7. Production Size Ceramic Waste Form Core Temperature Versus Time

## 5. Model 2 Results

Model 2 was developed to provide temperature profiles and densification data to correlate with experimental data. Fig. 8 and Fig. 9 illustrate the temperature profiles and densification predictions for a 25 kg CWF, respectively.

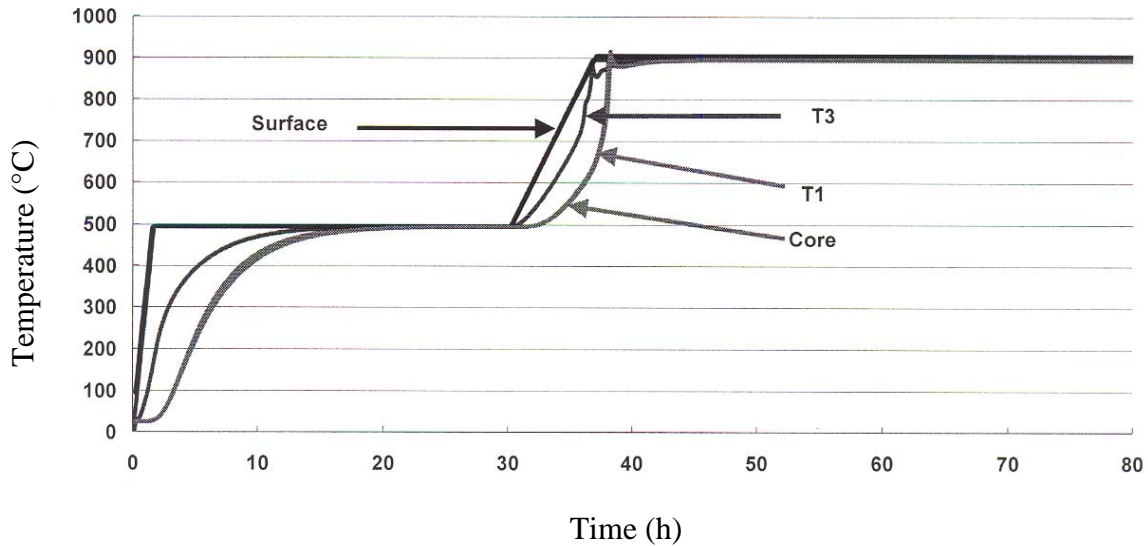


Fig. 8. Temperature Versus Time for 25 kg Ceramic Waste Form Model

Fig. 8 shows the predictions for temperatures at the thermocouple (TC) locations used in the 25 kg experiment. As shown in Fig. 1a, T1 represents the temperature 15.25 cm up from the can bottom in the radial center of the can. T3 represents the temperature 15.25 cm up from the can bottom and 8.9 cm from the radial center of the can. The surface temperature was the set-point temperature used by the furnace controller. The core temperature was a prediction of the temperature of the core of the material and moved during consolidation. There was no thermocouple in the experiment to track this temperature. This data indicates that the “true” moving core temperature, which would be difficult to track during an experiment, could be represented with a fixed center thermocouple during the experiment. The model also depicts the gradient that exist radially and also shows an exothermic reactions in all locations.

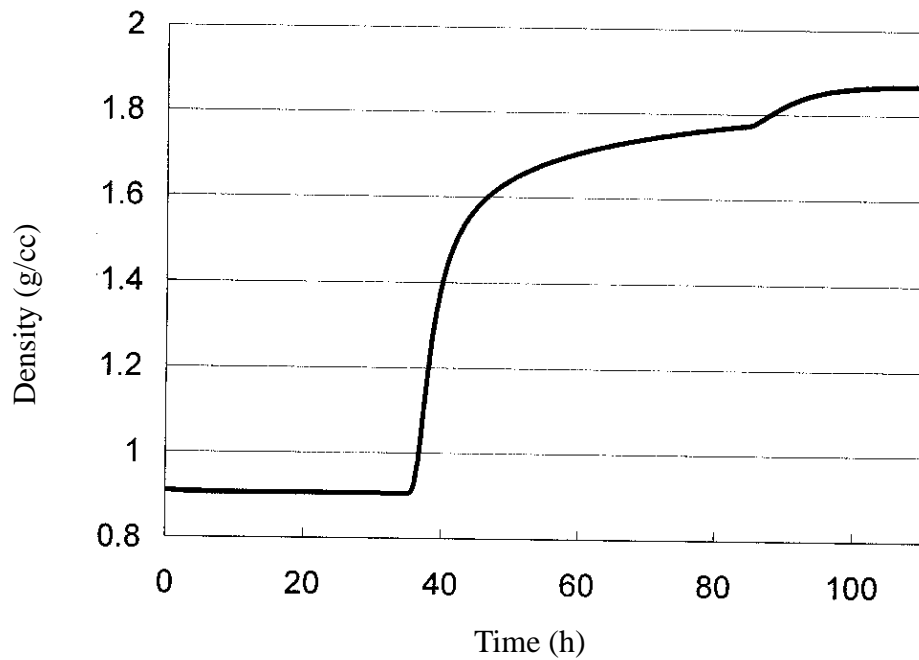


Fig. 9. Bulk Density Versus Time for the 25 kg Ceramic Waste Form Model

Fig. 9 shows the bulk density versus time predicted by the model. It is important to note that the density represented is an average density, not a point density. An average density is desired as it can be compared to experimental results obtained from the linear potentiometer. During the first 35 hours no increase in density was observed. Initial densification occurred rapidly, then asymptotically approached the maximum density. As can be seen at around 80 hours, cooling also produced a density increase due to the thermal contraction of the material.

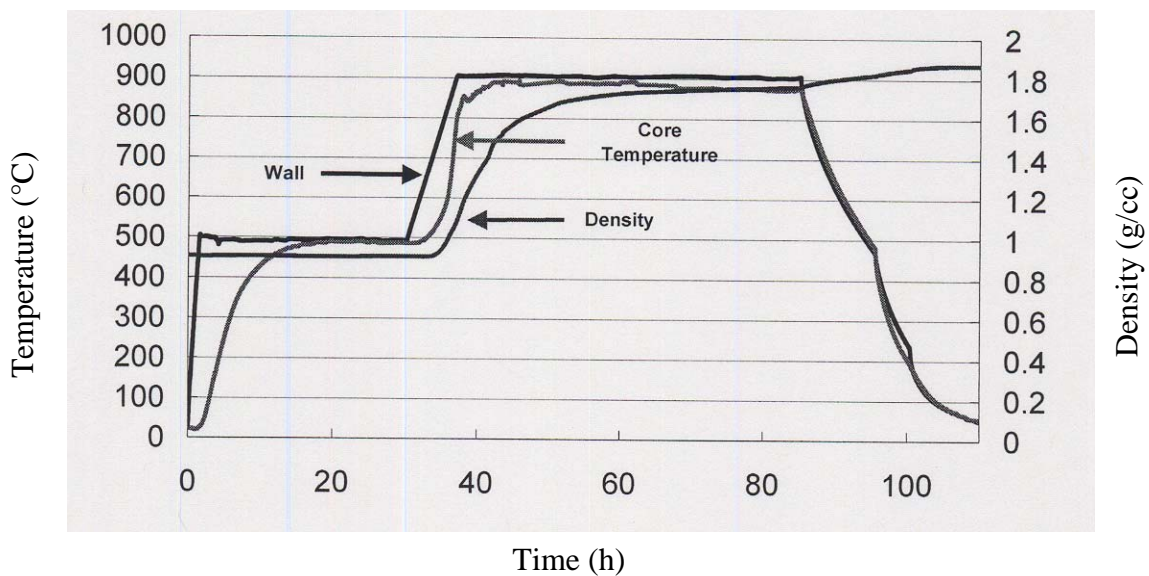


Fig. 10. Experimental Data from 25 kg Ceramic Waste Form Experiment

The temperature and density data obtained from a 25 kg CWF experiment is illustrated in Fig. 10. The two temperature readings refer to thermocouples placed on the wall of the canister and in the radial center (TC1) of the canister. The density plot was obtained by using the linear potentiometer readings to calculate height and bulk density. The data from the experiment can be plotted with the model data and the accuracy of Model 2 can be observed. This overlay of data is shown in Fig. 11 and Fig. 12. Figure 11 shows the temperature overlays, while Fig. 12 shows the density overlays. As is shown in Fig. 11, the model accurately predicts the initial heat up to 500°C. During this part of the experiment, any remaining moisture was driven off as the material is heated. The model assumption of 150% increase in the thermal conductivity seems to be validated. During the 500°C soak, the temperature of material equalized; this is accurately reflected by the model. After the soak, the prediction by the model correlates as temperature increases, however, using the current parameters, the model was unable to predict the rapid heating associated with the exothermic reaction. The overall modeled trend, however, is representative of the experimental results.

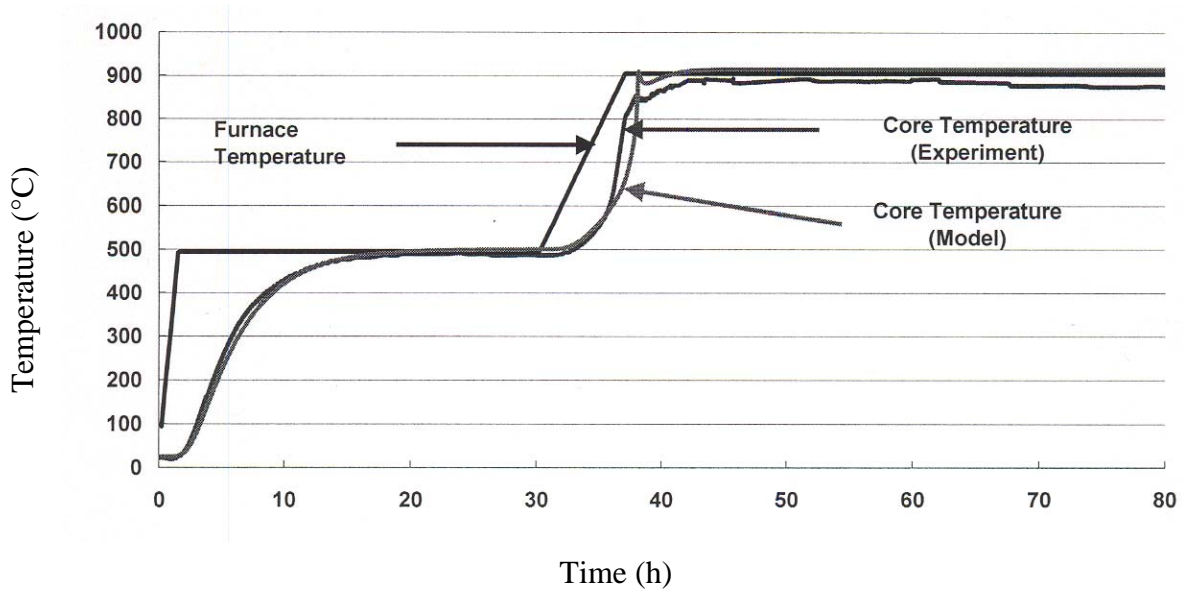


Fig. 11. Comparison of Model 2 Versus 25 kg Experimental Temperature Data

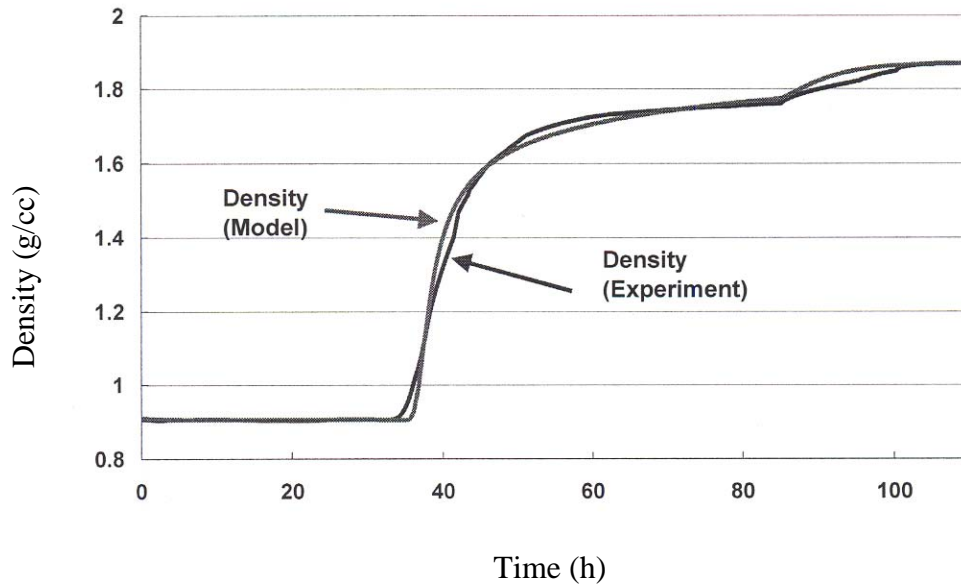


Fig. 12. Comparison Model 2 Versus 25 kg Experimental Bulk Density Data

Fig. 12 shows comparisons between the model's predictions of bulk density and the actual experimental data. As the material was heated, both the modeled and the experimental data remained at constant density. The model accurately tracked the rapid densification as the bulk temperature approached 567°C. The model continues to track the experiment during the long 915°C hold. The model also appeared to predict the thermal contraction of the material as it cooled at around 80 h. The model predicted a final density of 1.85 g/cm<sup>3</sup>, whereas the experiment yielded a final density of 1.87 +/- 0.02 g/cm<sup>3</sup>.

An experimental setup similar to the 25 kg sample was used to produce a 140 kg sample. The results of the model are compared to the experimental data in Fig. 13 and Fig. 14. The temperature plot (Fig. 13) shows data from a center thermocouple, located 6.2 in. from the bottom of the canister. As is shown, the model again looks very similar to the experimental data. At around 150 hours, an exothermic reaction created a spike in temperature. The model and the experiment behaved the same.

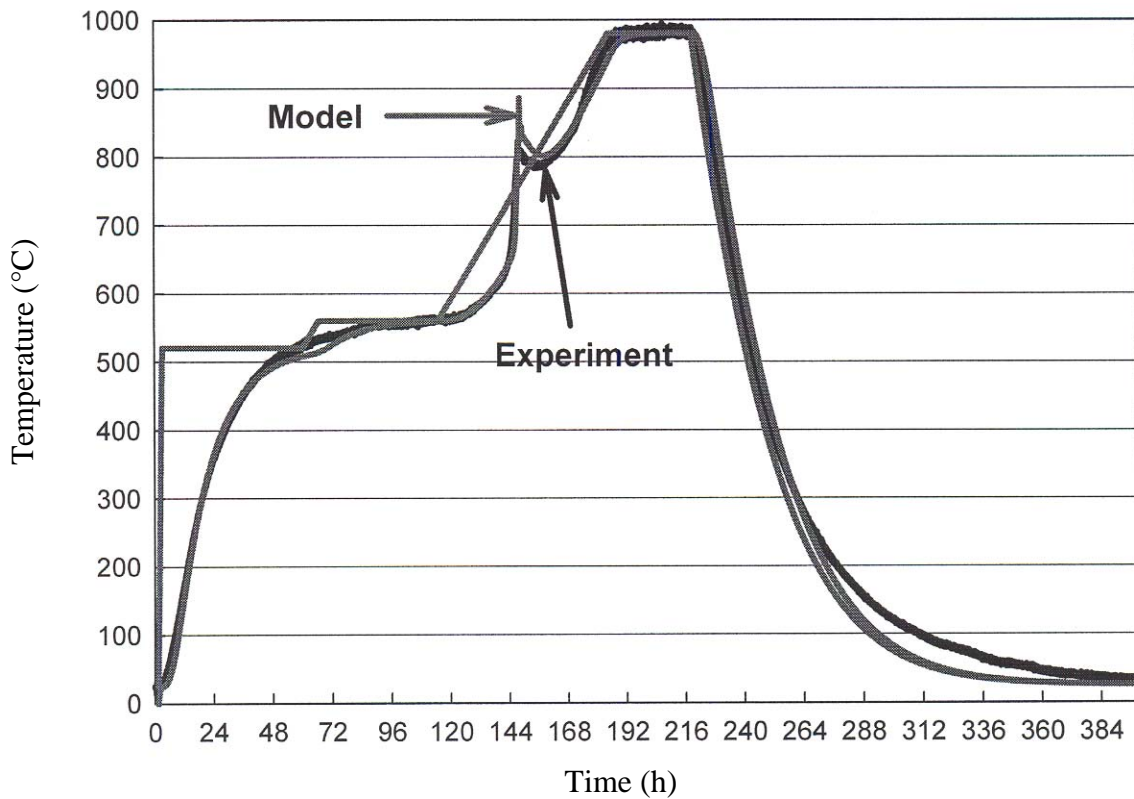


Fig. 13. Comparison of Model 2 Versus 140 kg Experimental Temperature Data

Fig. 14 shows that the model accurately predicted the general trends observed in the experimental density data. There appears to be a slight offset between the two sets of data. This deviation is most obvious in the data during the material heated up. The model shows that there was no increase in density, however, the experiment records a slight increase. This increase can be attributed to the thermal expansion of the 200 kg of steel that was used to maintain an inert environment. The model predicted the final bulk density to be  $2.0 \text{ g/cm}^3$ . The measured bulk density was  $1.98 \pm 0.02 \text{ g/cm}^3$ .

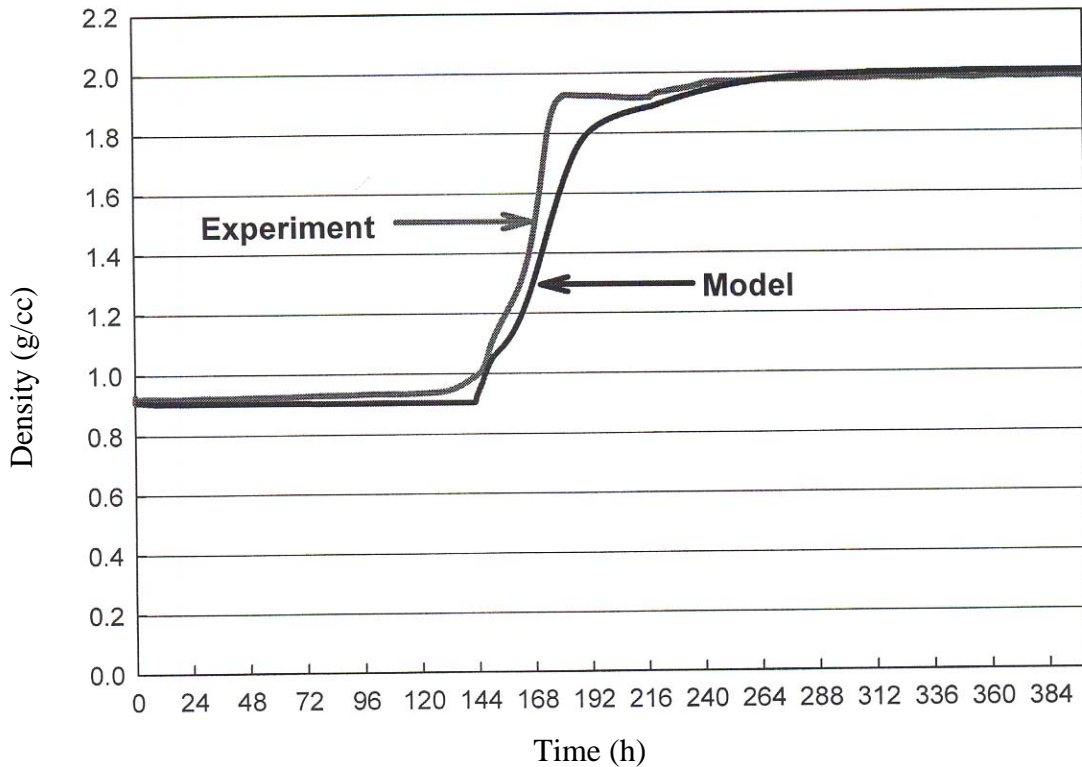


Fig. 14. Comparison of Model 2 Versus 140 kg Experimental Bulk Density Data

## 6. Conclusions

The results of the comparison between the experiments and model are very promising. The results from the first model bounded the canister height for a 200 kg CWF between 0.5 m to 1.0 m and bounded the hold time for the same mass between 12 and 70 h. The required hold time at maximum temperature for masses above 200 kg was shown to remain constant. The second model included variables that varied with temperature and time at temperature. The data from this model was found to accurately represent temperature trends observed within experimental CWFs. Additionally, the data was within 1% of the data for the bulk density of experimental CWFs up to 140 kg. The models were useful in determining processing conditions of CWFs and will continue to be a valuable tool during the scale-up CWFs.

## ACKNOWLEDGMENT

This work was supported by the U. S. Department of Energy, Office of Nuclear Energy, Science and Technology, under Contract W-31- 109-Eng-38 with the University of Chicago as operator of Argonne National Laboratory.

## REFERENCES

1. K. M. Goff, R. W. Benedict, K. J. Bateman, M. A. Lewis, C. Pereira, and C. A. Musick, "Spent Fuel Treatment and Mineral Waste Form Development at Argonne National Laboratory-West," 3:2436, American Nuclear Society, *International Topical Meeting On Nuclear And Hazardous Waste Management*, Seattle, WA (August 18-23, 1996).
2. M. C. Hash, A. S. Hebden, N. L. Stephenson, and M. Foubert to Distribution, Argonne National Laboratory-East, personal communication (July 2000).
3. MathCad 2001 is a registered trademark of Mathsoft, Inc., Copyright © 1986-2001, Cambridge, MA (2001).
4. F. P. Incropera and D. P. DeWitt, *Fundamentals of Heat and Mass Transfer*, 4<sup>th</sup> ed., 229-230, 243- 244, John Wiley & Sons, Inc., New York, NY (1996).
5. F. P. Incropera and D. P. DeWitt, *Fundamentals of Heat and Mass Transfer*, 4<sup>th</sup> ed., 248-249, John Wiley & Sons, Inc., New York, NY (1996).
6. O. Levenspiel, *Chemical Reaction Engineering*, 2<sup>nd</sup> ed., 50-51, John Wiley & Sons, Inc., New York, NY (1972).
7. "Thermophysical Properties of Seven Ceramic Materials" Thermophysical Properties Research Laboratory, Inc. Report (March 2001).

# APPENDIX A

Note: All inputs should include units where appropriate.

$$C := K \quad K_{el} := 273.15 \cdot K$$

### User Inputs: Physical Properties

Initial Density, found by initial measurements

$$\rho_i := .91 \frac{gm}{cm^3}$$

ref density, from TPRL report; represents a reference point used to fit data

$$\rho_{ref} := 2 \frac{gm}{cm^3}$$

### User Inputs: Model Properties

Container Radius measured value

$$R := \frac{20.9}{2} \text{ in}$$

End of model

$$t_{end} := 400 \text{ hr}$$

Softening point of glass from manufacturer specs

$$T_{ref} := 567 \cdot C$$

Mass of material, measured value

$$M := 140.21 \text{ kg}$$

Generation Term

$$q_{dot} := 0 \frac{kw}{tonne}$$

Initial thermal conductivity, has some variation but between .1 and .14

$$k_i := .135 \frac{W}{m \cdot K}$$

Number radial nodes, user choice, more nodes = better accuracy and more computing time counter begins at zero

$$a := 7$$

Furnace ramp up rate to Tf

$$T_{r2} := 0.1 \frac{C}{min}$$

Theoretical Density 2.3 for good material, MFD-02 is 2.15

$$\rho_{th} := 2.15 \frac{gm}{cm^3}$$

Coefficient of heat transfer during cool down, varies by furnace

$$h := 21 \frac{W}{m^2 \cdot K}$$

Initial temperature

$$T_i := 25 \cdot C$$

Hold time at Tint

$$t_{h1} := 112.2 \text{ hr}$$

Intermediate thermal conductivity (Guessed value of k at Tref)

$$k_{int} := 1.6 \cdot k_i$$

Ref thermal conductivity, at reference density (pref) from the TPRL report.

$$k_{ref} := 1.4 \frac{W}{m \cdot K}$$

Final temperature

$$T_f := 980 \cdot C$$

Furnace hold time at Tf

$$t_{h2} := 34 \text{ hr}$$

Coefficient of thermal expansion from TPRL report

$$\beta := 10^{-5} \frac{1}{K} \quad \beta_c := 4.75 \cdot 10^{-5} \frac{1}{K}$$

Atmospheric Pressure

$$P_{atm} := 12 \text{ psi}$$

Furnace ramp up rate to Tint

$$T_{r1} := 5 \frac{C}{min}$$

Heat of Reaction Constants Hr1 sets magnitude of heat, xHr sets rate of descent, default values of  $2.5 \times 10^8$  and .27. For old model performance set Hr1 to 1.

$$H_{r1} := 1.25 \cdot 10^8 \quad x_{Hr} := .27$$

Coordinates for set Point Temperatures

TC 1 Ra1 is distance from radial center, Z1 is height

$$Ra1 := 0 \text{ in} \quad Z1 := 3.1 \text{ in}$$

TC 2 Ra2 is distance from radial center, Z2 is height

$$Ra2 := 0 \text{ in} \quad Z2 := 6.2 \text{ in}$$

### Precalculated Inputs:

Preexponential rate constant

$$k_1 := 1 \times 10^{-5} \text{ Hz}$$

Activation Energy/Universal gas constant

$$E_1 := 3.942 \times 10^4 \text{ K}$$

Order of Reaction

$$n_g := 5.323$$

Order of temperature

$$\beta_g := 5.159$$

Coefficients of heat capacity curve

$$c := (-9.494 \cdot 10^6 \quad .535 \quad 772.318)$$

Note: All reaction constants (k1, E1, ng, βg) are derived in Mathcad work sheet "constants", Cp coefficients are found in work sheet "Cp curve fit"

$$c_1 := c \frac{T}{kg \cdot K}$$

### Calculations:

Cylinder Height

$$H := \frac{M}{\pi \cdot R^2 \cdot \rho_i} \quad H = 27.407 \text{ in} \\ H = 2.284 \text{ ft}$$

Number of vertical nodes

$$b := \text{floor} \left( a \frac{H}{R} \right) \quad b = 18$$

Final Height based on reference density.

$$H_{ref} := \frac{M}{\pi \cdot R^2 \cdot \rho_{ref}} \quad H_{ref} = 12.47 \text{ in}$$

Density of 1% Carbon Steel

$$\rho_{CS} := 7800 \frac{kg}{m^3} \quad \rho_{CS} = 0.282 \frac{lb}{in^3}$$

Desired PSI loading

$$PL := 1 \frac{lb}{in^2}$$

Plug Height for 1psi

$$PH := \frac{PL}{\rho_{CS}} \quad PH = 3.549 \text{ in}$$

Center Ring Height

$$HC := PH + H - 2 \cdot H_{ref} \quad HC = 6.015 \text{ in}$$

Mass of Plug  
 $MP := PH \cdot \rho CS (\pi \cdot R^2)$   
 $MP = 155.614 \text{ kg}$   
 $MP = 343.07 \text{ lb}$

Set Fourier number, for stability needs to be less than .25

$$Fo := \frac{1}{5}$$

Initial mass percent of zeolite/glass

$$X_0 := 1$$

Temperature dependent slope and intercept of k

$$sl := \frac{k_{int} - k_i}{T_{ref} - T_i} \quad int := k_i - sl \cdot T_i$$

Factor of k dependence on density, Doug's magic

$$fac := \frac{\rho_i (k_{ref} - k_i)}{k_i (p_{ref} - \rho_i)}$$

Total # of nodes

$$ab := (a + 1) \cdot (b + 1) \quad ab = 152$$

$$fac = 7.823$$

Distance between radial nodes

$$\Delta r := \frac{R}{a}$$

$$\Delta r = 1.493 \text{ in}$$

Distance between axial nodes (initially)

$$\Delta z := \frac{H}{b}$$

$$\Delta z = 1.523 \text{ in}$$

Radial area

$$Ar := \pi \cdot R^2$$

Range Variables

Temperature Initial Condition set to  $T_i$

$$i := 0..b \quad j := 0..a$$

$$T_{ic_{i,j}} := T_i$$

Thermal Diffusivity Initially

$$\alpha_i := \frac{k_i}{\left[ c_{l_0} \left( \frac{T_i + K_{el}}{K} \right)^{-2} + c_{l_1} \cdot \frac{T_i + K_{el}}{K} + c_{l_2} \right] \cdot \rho_i}$$

Radial distance of node j from core

$$r_j := R - j \cdot \Delta r$$

$$\alpha_i = 1.798 \times 10^{-7} \frac{\text{m}^2}{\text{s}}$$

Weight factor for averaging radial nodes to represent a 3D model

$$A_0 := \pi \cdot \left[ R^2 - \left( R - \frac{\Delta r}{2} \right)^2 \right]$$

$$i := 1..a - 1$$

$$A_i := \pi \cdot \left[ \left( r_i + \frac{\Delta r}{2} \right)^2 - \left( r_i - \frac{\Delta r}{2} \right)^2 \right]$$

$$A_a := \pi \cdot \left( \frac{\Delta r}{2} \right)^2$$

$$rat_{r_j} := \frac{A_j}{Ar} \cdot (2-a)^2$$

Weight factor for averaging axial nodes to represent a 3D model

$$rat_{z_0} := 1$$

$$\lambda := 1..b - 1$$

$$rat_{z_\lambda} := 2$$

$$rat_{z_b} := 1$$

Diameter

$$D := 2 \cdot R$$

Number of elements

$$num := a \cdot b$$

$$num = 126$$

Time step 1

$$\Delta t := \text{if} \left( \Delta z < \Delta r, \frac{Fo \cdot \Delta z^2}{\alpha_i}, \frac{Fo \cdot \Delta r^2}{\alpha_i} \right)$$

Total time

$$time := \Delta t$$

Time furnace reaches  $T_{int}$

$$t_{r1} := \frac{T_{int} - T_i}{T_{r1}} \quad t_{r1} = 1.783 \text{ hr}$$

Time furnace starts ramp2

$$t_2 := t_{r1} + t_{h1}$$

$$t_2 = 113.983 \text{ hr}$$

Time furnace reaches  $T_f$

$$t_f := \frac{T_f - T_{int}}{T_{r2}} + t_2$$

$$t_f = 183.983 \text{ hr}$$

Time furnace starts cool down

$$t_c := t_f + t_{h2}$$

$$t_c = 217.983 \text{ hr}$$

Surface temperature

$$T_s := \text{if} (time < t_f, T_i + T_{r1} \cdot time, T_f)$$

Rate constant

$$k_0 := \left[ k_1 \left( \frac{T_{ic} + K_{el}}{K} \right)^{\beta_g} \cdot \exp \left( \frac{-E_1}{T_{ic} + K_{el}} \right) \right]$$

Mass Percent of Zeolite Glass

$$X := \left[ X_0^{1-n_g} + k_0 \cdot \Delta t \cdot (n_g - 1) \right]^{1-n_g}$$

Density

$$\rho := \left[ \frac{\rho_i}{\beta \cdot (T_{ic} - T_i) + 1} \left[ 1 + \left( \frac{\rho_{th}}{\rho_i} - 1 \right) \cdot (1 - X) \right] \right]$$

Thermal conductivity

$$k := \frac{\text{fac} \cdot k_i \cdot (\rho - \rho_i)}{\rho_i} + T_{ic} \cdot sl + \text{int}$$

Heat Capacity

$$C_p := \left[ c_{10} \cdot \left( \frac{T_{ic} + \text{Kel}}{K} \right)^{-2} + c_{11} \cdot \frac{T_{ic} + \text{Kel}}{K} + c_{12} \right]$$

Average Density

$$\rho_{ave} := \frac{\sum_{j=0}^a \sum_{i=0}^b \rho_{i,j} \cdot \text{rat}_j \cdot \text{rat}_i}{\sum_{j=0}^a \sum_{i=0}^b \text{rat}_j \cdot \text{rat}_i} \quad \rho_{ave} = 910 \frac{\text{kg}}{\text{m}^3}$$

Recalculated Height, distance between axial nodes, and thermal diffusivity after time step 1

$$H := \frac{M}{\pi \cdot R^2 \cdot \rho_{ave}} \quad \Delta z := \frac{H}{b} \quad \alpha := \frac{k}{\rho \cdot C_p}$$

Temperature, density, heat capacity, thermal conductivity, height, etc. will be recalculated at each time step until tend is reached using the following hidden program.



```

Return :=
  i ← 1
  O ← 0
  t_0 ← time
  T_0 ← T_ic
  T_sur_0 ← T_s
  X_1_0 ← X
  ρ_1_0 ← ρ
  ρ_tot_0 ← ρ_ave
  k_1_0 ← k
  C_p_1_0 ← C_p
  α_1_0 ← α
  Δt_0 ← Δt
  while t_{i-1} < tend
    k_00 ←  $\left[ k_1 \cdot \left( \frac{T_{i-1} + \text{Kel}}{K} \right)^{\beta_g} \cdot \exp \left( \frac{-E_1}{T_{i-1} + \text{Kel}} \right) \right]$ 
    X_1_i ←  $\left[ (X_{1_{i-1}})^{1-n_g} + k_{00} \cdot \Delta t_{i-1} \cdot (n_g - 1) \right]^{\frac{1}{1-n_g}}$ 
    while t_{i-1} ≥ t_c ∧ O = 0
      c ← i - 2
      O ← 1
  
```

$$\rho_2 \leftarrow \left[ \frac{\rho_i}{\beta \cdot (T_{i-1} - T_c) + 1} \cdot \left[ 1 + \left( \frac{\rho_{th}}{\rho_i} - 1 \right) \cdot (1 - X_{1i}) \right] \right]$$

$$\rho_1 \leftarrow \text{if} \left[ t_{i-1} < t_c, \rho_2, \frac{\rho_2}{\beta \cdot (T_{i-1} - T_c) + 1} \right]$$

$$k1_i \leftarrow \left[ \frac{(\rho_1 - \rho_i)}{\rho_i} + \text{int} + \text{sl} \cdot T_{i-1} \right]$$

$$C_{p1_i} \leftarrow \left[ c1_0 \left( \frac{T_{i-1} + \text{Kel}}{K} \right)^{-2} + c1_1 \frac{T_{i-1} + \text{Kel}}{K} + c1_2 \right]$$

$$\rho_{tot_i} \leftarrow \frac{\sum_{i=0}^b \sum_{j=0}^a (\rho_1)_{i,j} \cdot \text{rat}_{r_j} \cdot \text{rat}_{z_i}}{\sum_{i=0}^b \sum_{j=0}^a \text{rat}_{r_j} \cdot \text{rat}_{z_i}}$$

$$He \leftarrow \frac{M}{\pi \cdot R^2 \cdot \rho_{tot_i}}$$

$$\Delta ze \leftarrow \frac{He}{b}$$

$$\text{Height}_0 \leftarrow \Delta z$$

$$\text{Height}_i \leftarrow \Delta ze$$

for  $i \in 0..b$

$$\left\{ \begin{array}{l} z_i \leftarrow He - i \cdot \Delta ze \\ P_i \leftarrow \rho_{tot_i} \cdot g \cdot (He - z_i) + P_{atm} \end{array} \right.$$

$$\alpha 1_i \leftarrow \frac{k1_i}{\rho 1_i \cdot C_{p1_i}}$$

$$\Delta t_i \leftarrow \text{if} \left[ \Delta ze < \Delta r, \frac{Fo \cdot \Delta ze^2}{\max(\alpha 1_i)}, \frac{Fo \cdot \Delta r^2}{\max(\alpha 1_i)} \right]$$

$$T_{sur_i} \leftarrow \text{if} \left[ t_{i-1} < t_{r1}, T_i + T_{r1} \cdot t_{i-1}, \text{if} \left[ t_{i-1} < t_{r2}, T_{int}, \text{if} \left[ t_{i-1} < t_f, T_{int} + T_{r2} \cdot (t_{i-1} - t_{r2}), \text{if} \left[ t_{i-1} < t_c, T_f \cdot (T_{sur_{i-1}} - T_i) \cdot \exp \left[ \left[ \frac{h}{(\rho 1)_{0,0} \cdot (C_{p1})_{0,0}} \right] \cdot \Delta t_i \right] + T_i \right] \right] \right] \right]$$

for  $i \in 0..b$

for  $j \in 0..a$

$$T2_{i,j} \leftarrow \text{if} \left[ i = 0 \vee j = 0 \vee i = b, T_{sur_i}, (\alpha 1)_{i,j} \cdot \Delta t_i \cdot \left[ \text{if} \left[ j = a, \frac{(T_{i-1})_{i-1,j} + (T_{i-1})_{i+1,j} - 2(T_{i-1})_{i,j}}{2} \dots \frac{(T_{i-1})_{i-1,j} + (T_{i-1})_{i+1,j} - 2(T_{i-1})_{i,j}}{2} \dots \right] + 1 \right. \right. \\ \left. \left. + 2 \frac{(T_{i-1})_{i,j-1} - 2(T_{i-1})_{i,j}}{2} \dots \frac{(T_{i-1})_{i,j-1} + (T_{i-1})_{i,j+1} - 2(T_{i-1})_{i,j}}{2} \dots \right] \right]$$

$$\begin{aligned}
 & \left[ \begin{aligned}
 & + P_i \frac{\text{Height}_{i-1} - \text{Height}_i}{(k1)_{i,j} \cdot \text{Height}_i \cdot \Delta t_i} \dots \\
 & + \left[ \frac{\rho_i - (\rho1)_{i,j}}{\text{xHr}(\rho1)_{i,j} + 1} \right] \left[ (X_{1-i})_{i,j} - (X_{1i})_{i,j} \right] \frac{K}{m^2} \dots \\
 & + \frac{\text{qdot}(\rho1)_{i,j}}{(k1)_{i,j}}
 \end{aligned} \right] \\
 & \left[ \begin{aligned}
 & + \frac{1}{r_j} \frac{(T_{1-i})_{i,j-1} - (T_{1-i})_{i,j+1}}{2 \cdot \Delta r} \dots \\
 & + P_i \frac{\text{Height}_{i-1} - \text{Height}_i}{(k1)_{i,j} \cdot \text{Height}_i \cdot \Delta t_i} \dots \\
 & + \left[ \frac{\rho_i - (\rho1)_{i,j}}{\text{xHr}(\rho1)_{i,j} + 1} \right] \left[ (X_{1-i})_{i,j} - (X_{1i})_{i,j} \right] \frac{K}{m^2} \dots \\
 & + \frac{\text{qdot}(\rho1)_{i,j}}{(k1)_{i,j}}
 \end{aligned} \right]
 \end{aligned}$$

$T_1 \leftarrow T_2$   
 $\gamma_1 \leftarrow \begin{cases} i \leftarrow 0 \\ \text{while } z_1 > Z1 \\ \quad i \leftarrow i + 1 \\ \quad i \end{cases}$   
 $\delta_1 \leftarrow \begin{cases} j \leftarrow 0 \\ \text{while } r_j > Ra1 \\ \quad j \leftarrow j + 1 \\ \quad j \end{cases}$   
 $\text{facz1} \leftarrow \text{if} \left[ \gamma_1 = 0, 0, \frac{Z1 - z_1}{\Delta z} \right]$   
 $\text{facr1} \leftarrow \text{if} \left[ \delta_1 = 0, 0, \frac{Ra1 - r_{\delta_1}}{\Delta r} \right]$   
 $Tz11 \leftarrow \text{if} \left[ \gamma_1 = 0, (T_{\gamma_1, \delta_1})_{\gamma_1, \delta_1} + [(T_{\gamma_1-1, \delta_1})_{\gamma_1-1, \delta_1} - (T_{\gamma_1, \delta_1})_{\gamma_1, \delta_1}] \cdot \text{facz1} \right]$   
 $Tz21 \leftarrow \text{if} \left[ \gamma_1 = 0 \vee \delta_1 = 0, (T_{\gamma_1, \delta_1})_{\gamma_1, \delta_1-1} + [(T_{\gamma_1-1, \delta_1-1})_{\gamma_1-1, \delta_1-1} - (T_{\gamma_1, \delta_1-1})_{\gamma_1, \delta_1-1}] \cdot \text{facz1} \right]$   
 $Tp1 \leftarrow Tz11 + (Tz21 - Tz11) \cdot \text{facr1}$   
 $\gamma_2 \leftarrow \begin{cases} i \leftarrow 0 \\ \text{while } z_1 > Z2 \\ \quad i \leftarrow i + 1 \\ \quad i \end{cases}$   
 $\delta_2 \leftarrow \begin{cases} j \leftarrow 0 \\ \text{while } r_j > Ra2 \\ \quad j \leftarrow j + 1 \\ \quad j \end{cases}$   
 $\text{facz2} \leftarrow \text{if} \left[ \gamma_2 = 0, 0, \frac{Z2 - z_2}{\Delta z} \right]$

$$\begin{aligned}
 & \text{facr2} \leftarrow \text{if} \left[ \delta 2 = 0, 0, \frac{Ra2 - r_{\delta 2}}{\Delta r} \right] \\
 & Tz12 \leftarrow \text{if} \left[ \gamma 2 = 0, (T_{i, \gamma 2, \delta 2}, (T_{i, \gamma 2, \delta 2} + [(T_{i, \gamma 2-1, \delta 2} - (T_{i, \gamma 2, \delta 2})] \cdot \text{facz2}]) \right. \\
 & Tz22 \leftarrow \text{if} \left[ \gamma 2 = 0 \vee \delta 2 = 0, (T_{i, \gamma 2, \delta 2}, (T_{i, \gamma 2, \delta 2-1} + [(T_{i, \gamma 2-1, \delta 2-1} - (T_{i, \gamma 2, \delta 2-1})] \cdot \text{facz2}]) \right. \\
 & Tp2_i \leftarrow Tz12 + (Tz22 - Tz12) \cdot \text{facr2} \\
 & t_i \leftarrow t_{i-1} + \Delta t_i \\
 & i \leftarrow i + 1
 \end{aligned}$$

$$\left( \begin{array}{l}
 \rho_{\text{tot}} \cdot \frac{\text{m}^3}{\text{kg}} \\
 t \\
 \frac{t}{s} \\
 \frac{T}{K} \\
 C_{p1} \cdot \frac{\text{kg} \cdot K}{J} \\
 k1 \cdot \frac{\text{m} \cdot K}{W} \\
 \rho1 \cdot \frac{\text{m}^3}{\text{kg}} \\
 \frac{Tp1}{K} \\
 \frac{Tp2}{K} \\
 i - 1 \\
 \alpha1 \cdot \frac{s}{\text{m}^2}
 \end{array} \right)$$



With an assumption of 2D axisymmetric analysis, the heat diffusion equation in cylindrical coordinates becomes:

$$\frac{1}{\alpha} \frac{\partial}{\partial t} T = \frac{1}{r} \frac{\partial}{\partial r} \left( r \cdot \frac{\partial}{\partial r} T \right) + \frac{\partial^2}{\partial z^2} T + \frac{\dot{q}}{k}$$

Defining the integer p as the sequential time step where n is the number of time steps:

$$p = 1..n$$

Making an approximation using finite difference and utilizing the definition of p

$$\frac{\partial}{\partial t} T = \frac{(T_{p+1})_{i,j} - (T_p)_{i,j}}{\Delta t}$$

$$\frac{1}{\alpha} \cdot \frac{(T_{p+1})_{i,j} - (T_p)_{i,j}}{\Delta t} = \frac{(T_p)_{i+1,j} + (T_p)_{i-1,j} - 2(T_p)_{i,j}}{\Delta z^2} + \frac{(T_p)_{i,j+1} + (T_p)_{i,j-1} - 2(T_p)_{i,j}}{\Delta r^2} + \frac{1}{r} \cdot \frac{(T_p)_{i,j-1} - (T_p)_{i,j+1}}{2\Delta r} + \frac{\dot{q}}{k}$$

Which upon rearrangement becomes:

$$(T_{p+1})_{i,j} = \alpha \cdot \Delta t \cdot \left[ \frac{(T_p)_{i+1,j} + (T_p)_{i-1,j} - 2(T_p)_{i,j}}{\Delta z^2} + \frac{(T_p)_{i,j+1} + (T_p)_{i,j-1} - 2(T_p)_{i,j}}{\Delta r^2} + \frac{1}{r} \cdot \frac{(T_p)_{i,j-1} - (T_p)_{i,j+1}}{2\Delta r} + \frac{\dot{q}}{k} \right] + (T_p)_{i,j}$$

Where  $T(p)$  = Temperature at time step  $p$  and  $t$  and  $\Delta t$  represent time and time step respectively. The subscripts  $i$  and  $j$  are used to designate the nodal position in the  $z$  and  $r$  directions within the cylindrical coordinate system.

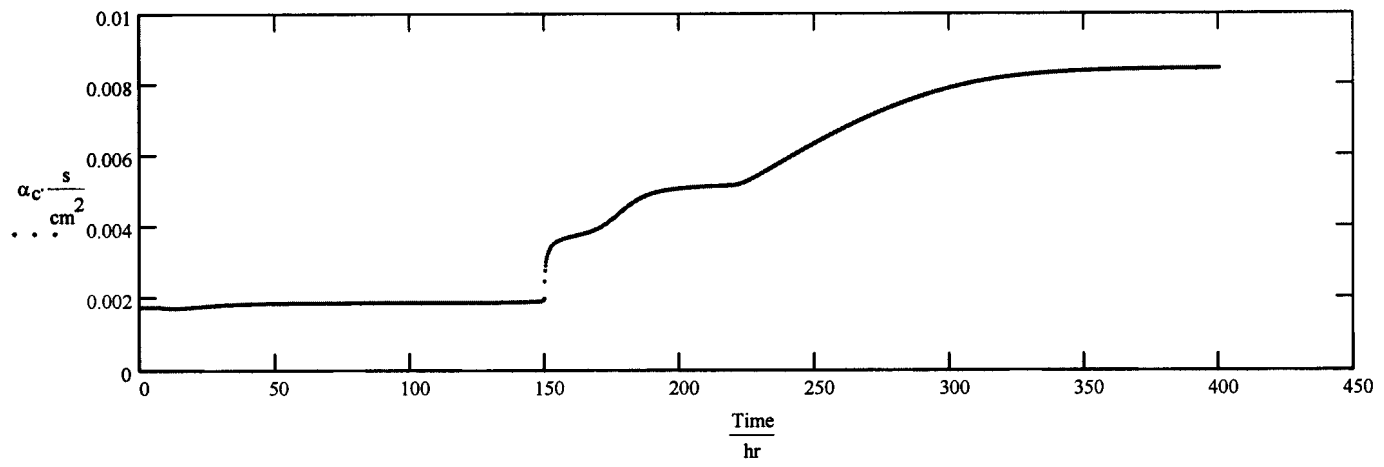
**Output:**

# Time Steps	Time Step Counter	Temperature Profile	Density Profile	Core Coordinate	Thermal Diffusivity
$n := \text{Return}_8$	$n = 9.652 \times 10^3 \quad p := 0..n$	$T_p := \text{Return}_2 \cdot C$	$\rho := \text{Return}_5 \cdot \frac{\text{kg}}{\text{m}^3}$	$c := \text{floor}\left(\frac{b}{2}\right)$	$\alpha := \text{Return}_5$

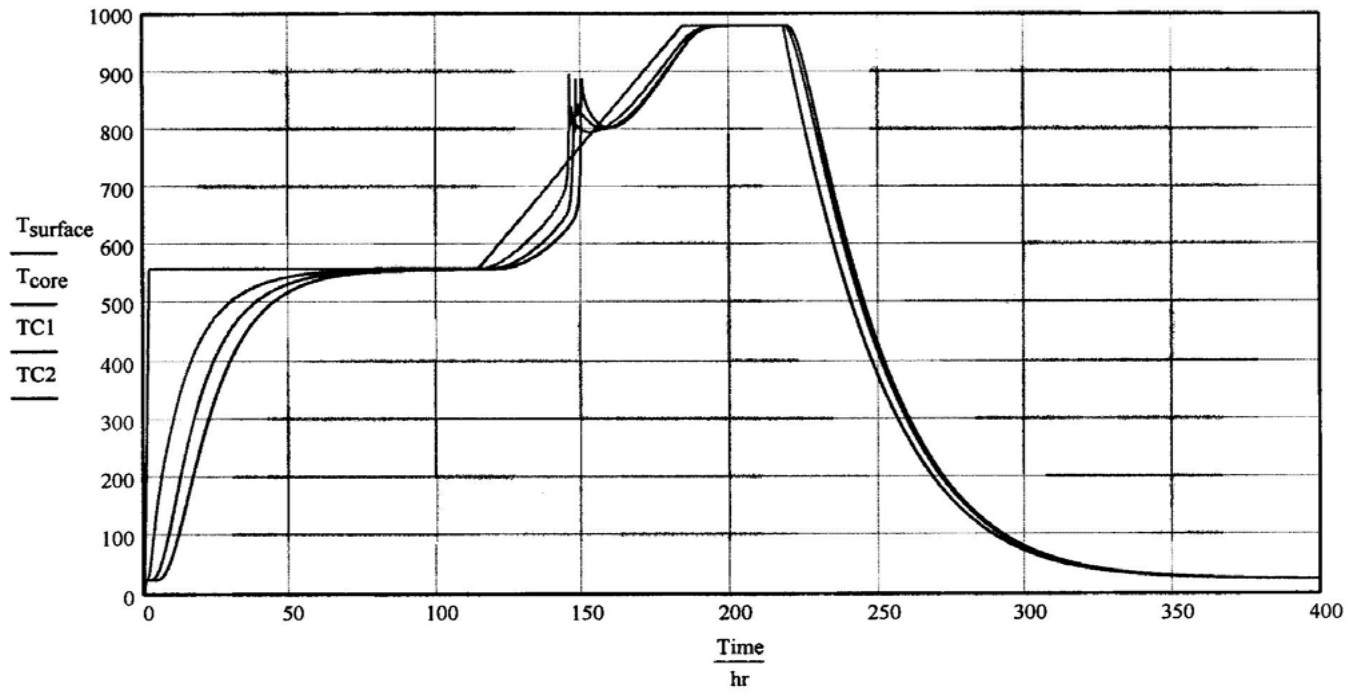
Average Density	Height of CWF	Core Temperature	Surface Temperature	Heat Capacity	Thermal Conductivity
$\rho_{ave} := \text{Return}_0 \cdot \frac{\text{kg}}{\text{m}^3}$	$\text{Height} := \frac{M}{\pi \cdot R^2 \cdot \rho_{ave}}$	$T_{core_p} := (T_p)_{c,a}$	$T_{surface_p} := (T_p)_{0,0}$	$C_p := \text{Return}_3 \cdot \frac{\text{J}}{\text{kg} \cdot K}$	$k := \text{Return}_4 \cdot \frac{\text{W}}{\text{m} \cdot K}$
Final Density	Final Height	Core Density	Surface Density	Final distance between axial nodes	
$\rho_f := \rho_{ave_n}$	$H_f := \frac{M}{\pi \cdot R^2 \cdot \rho_f}$	$\rho_{c_p} := (\rho_p)_{c,a}$	$\rho_{s_p} := (\rho_p)_{0,0}$	$\Delta z_f := \frac{H_f}{2 \cdot b}$	
Time	Point 1 Temperature	Point 2 Temperature	Thermal Diffusivity at Core	Thermal Conductivity at Core	
$\text{Time} := \text{Return}_1 \cdot s$	$\text{TC1} := \text{Return}_6 \cdot C$	$\text{TC2} := \text{Return}_7 \cdot C$	$\alpha_{c_p} := (\alpha_p)_{c,a}$	$k_{c_p} := (k_p)_{c,a}$	

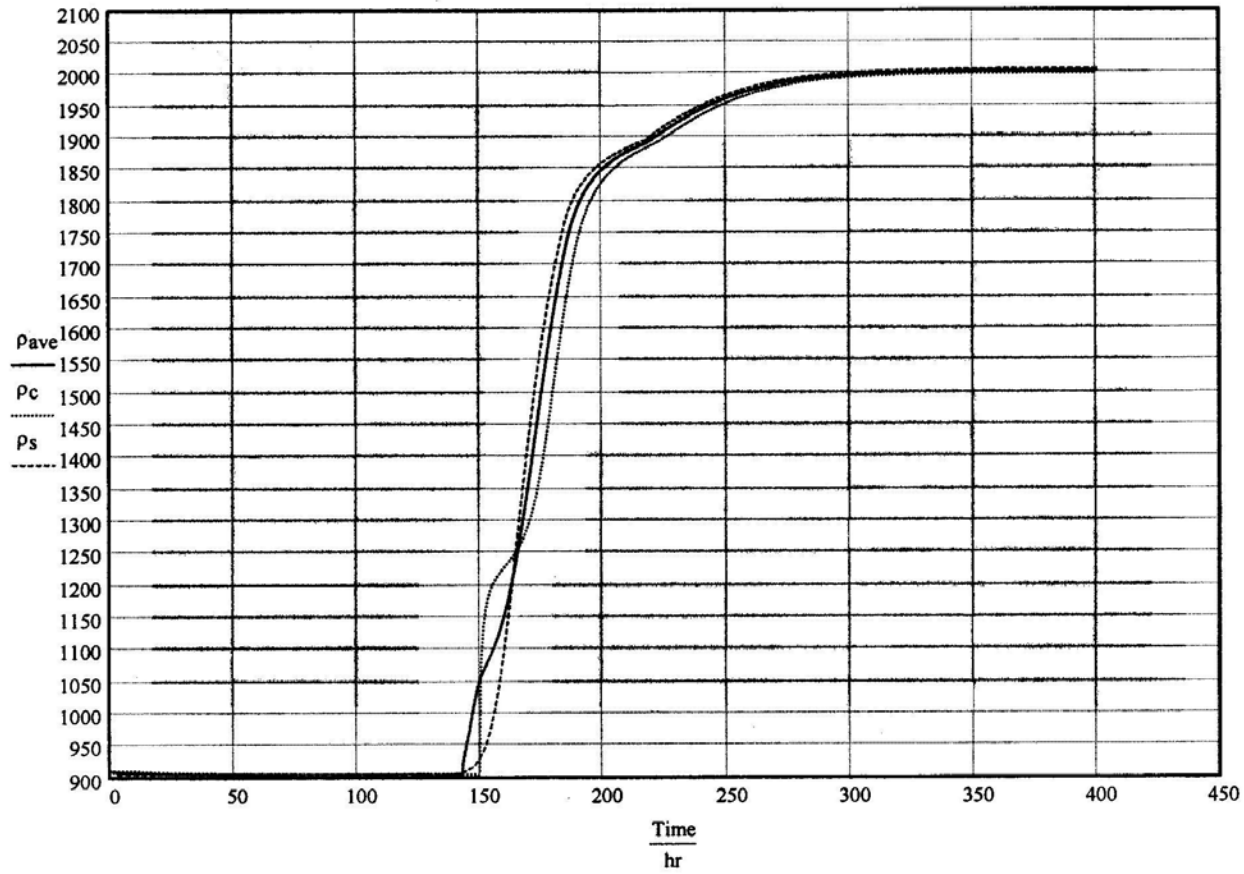
Heat Capacity at Core

```
T(M) :=  
  i ← a  
  M3 ← M  
  while i ≥ 1  
    M2 ← augment(M3, M3(i-1))  
    M3 ← M2  
    i ← i - 1  
  M2T
```



Plots:





$$\max(\rho_{ave}) = 2.003 \times 10^3 \frac{\text{kg}}{\text{m}^3}$$

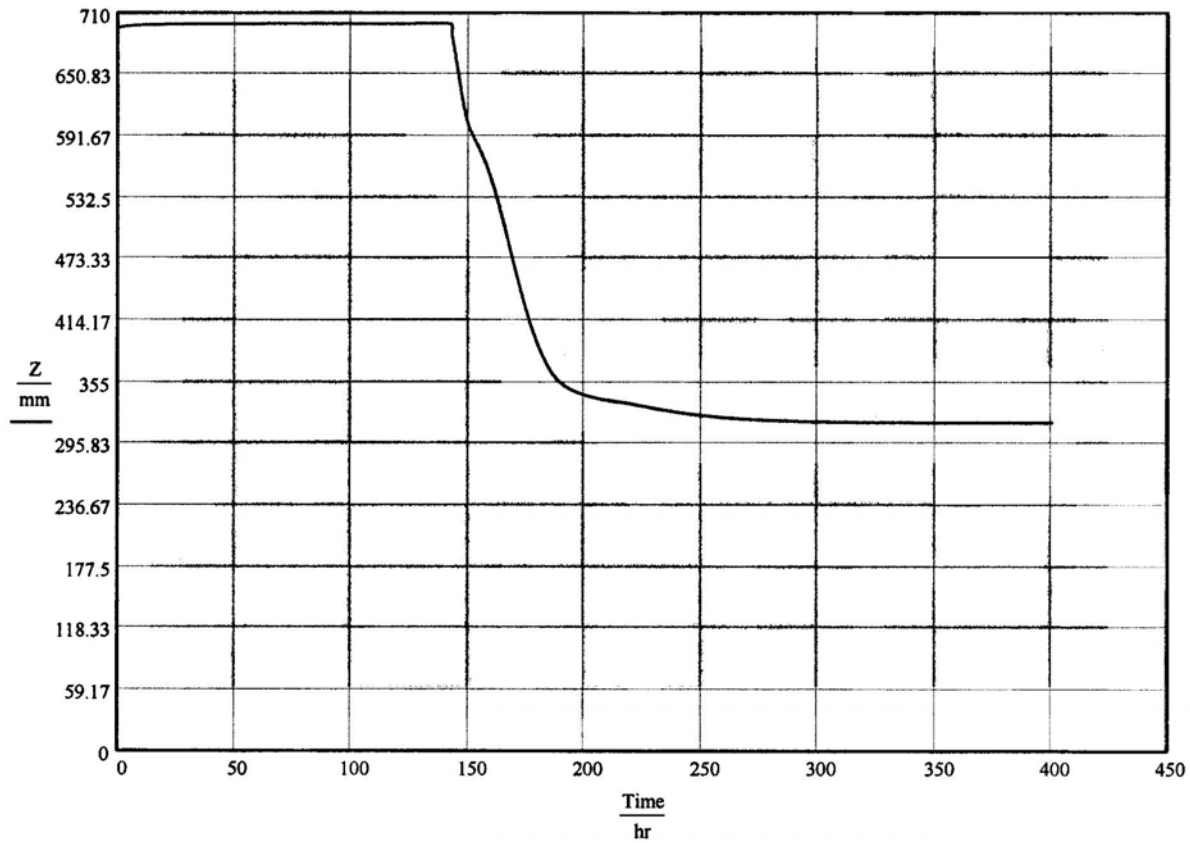
$$\max(T_{core}) = 979.999\text{C}$$

$$H = 27.407 \text{ in}$$

$$H_z := H \quad H_z = 27.407 \text{ in}$$

$$H_b := 76.938 \text{ in}$$

$$Z := \overbrace{(\text{Height} - \text{Height}_0 + H_z)}$$



$$\max(Z) = 700.314 \text{ mm}$$

$$\min(Z) = 316.261 \text{ mm}$$

$T_{\text{surface}} =$

	0
0	25
1	158.269
2	291.537
3	424.806
4	556.88
5	560
6	560
7	560
8	560
9	560
10	560
11	560
12	560
13	560
14	560
15	560

K

Time =

	0
0	26.654
1	53.307
2	79.961
3	106.376
4	132.052
5	157.027
6	181.986
7	206.945
8	231.904
9	256.863
10	281.822
11	306.781
12	331.74
13	356.699
14	381.659
15	406.618

min

$\rho_{\text{pave}} =$

	0
0	0.91
1	0.91
2	0.91
3	0.909
4	0.909
5	0.909
6	0.908
7	0.908
8	0.908
9	0.908
10	0.908
11	0.908
12	0.908
13	0.908
14	0.907
15	0.907

$\frac{\text{gm}}{\text{cm}^3}$

$T_{\text{core}} =$

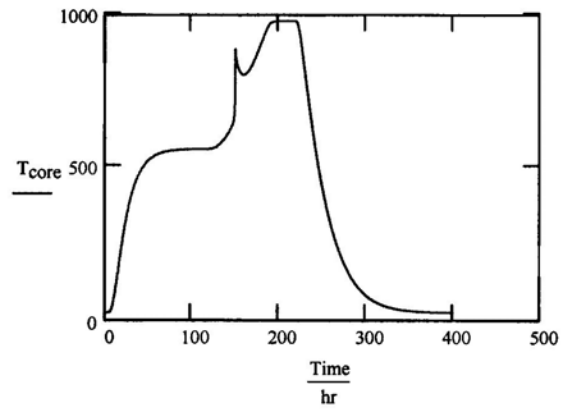
	0
0	25
1	25
2	25
3	25
4	25
5	25
6	25
7	25
8	25.014
9	25.085
10	25.28
11	25.699
12	26.448
13	27.626
14	29.311
15	31.555

K

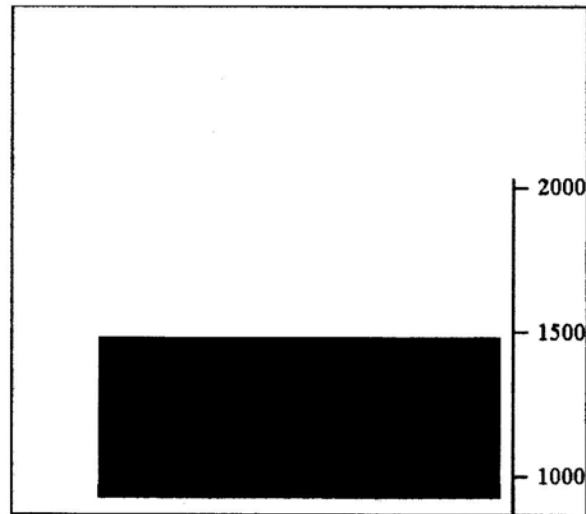
TCI =

	0
0	0
1	25
2	25
3	29.704
4	39.798
5	54.75
6	74.42
7	94.702
8	114.039
9	131.969
10	148.461
11	163.666
12	177.783
13	191.007
14	203.501
15	215.395

K



$$n = 9.652 \times 10^3$$



$T(T_{PFRAME}), T(P_{FRAME})$

$u := 1..n$

$tstep_u := Time_u - Time_{u-1}$

$tstep_0 := tstep_1$

